THERMAL AND MECHANICAL DAMAGE OF PBX'S

Gert Scholtes, Richard Bouma, Frans Peter Weterings, Albert van der Steen TNO Prins Maurits Laboratory P.O. Box 45, 2280 AA Rijswijk The Netherlands

Scholtes@pml.tno.nl

The TNO Prins Maurits Laboratory, has conducted research in energetic material response to several Insensitive Munition (IM) stimuli like cook-off, bullet-fragment impact and shaped charge impact. In addition to the development of highly instrumented test set-ups, predictive computer codes are also in development.

The response of energetic materials to these stimuli, depend strongly on the properties of these materials at onset and during an event. To understand the mechanisms and the parameters influencing the response, these materials have been tested in laboratory scale experiments.

The mechanical properties have been measured as a function of the strain rate (0.001 m/s-5m/s), in the temperature range from -60 up to 60°C . In addition to tensile-strength testing, relaxation testing for the same temperature range, has been performed. These experiments determine the Poisson ratio and time-temperature dependence of the mechanical properties of the explosive at intermediate and high strain rates impact, at ambient temperatures (rates that can be found in experiments like the gas gun and bullet/fragment impact experiments). Optical microscopy as well as scanning electron microscopy has been used to examine the samples after impact. The information is then used in the erosion/damage models for Autodyn calculations.

To assess thermal damage, mechanical properties have been measured as a function of the temperature (up to 160° C) and as a function of the degree of decomposition. These parameters will be used in cook-off computer models, to couple the thermal-chemical behaviour to the mechanical response. Also, laboratory scale experiments, shock initiation and fragment impact tests have been performed with damaged material. An overview of the research is presented in this paper.

INTRODUCTION

The TNO-PML laboratory has conducted research in IM, to understand the mechanisms that lead to the response and determine the parameters that have a major influence on sensitivity. Tests have been developed to analyse the mechanisms and computer codes are under develop-

ment to simulate the processes. For all the mechanisms of the different IM tests, mechanical properties and damage play a major role in the process that lead to a detonation response (type I or II response) or a less violent reaction (type III, IV or V response). Others have also investigated the influence of damage on the sensitivity of composites ^{1-4, 7}.

The mechanical properties of an energetic material play a major role in the mechanisms of SDT, DDT and XDT, all leading to a detonation. The SDT (Shock-to-Detonation Transition) phenomenon is relatively well understood. It is generally known that parameters like the critical diameter, shock Hugoniot, impact velocities and dimensions and properties of the impact threat, have an influence on this phenomenon. Although it is understood that ignition sites play a major role in the shock sensitivity, a quantitative relation between material properties, such as porosity, amount of inclusions, damage etc., and shock sensitivity is still not well understood. In DDT and XDT process, material properties like mechanical properties and damage play an even greater role (in such a way that it can lead to a range of reaction behaviour).

Several years ago, the research in mechanical properties and damage, influencing the sensitivity of an explosive, was started. After the preliminary studies, this resulted into research explosives like HU-43 and 44. Building on these preliminary studies, a new approach has been developed, to determine a quantitative relation between mechanical properties, thermal and mechanical damage and the sensitivity of an explosive to IM-like threats. This work presents this new approach.

PRODUCTION OF RESEARCH PBXS

Several RDX and HMX-PBXs have been produced and used in tests to access shock initiation, cook-off and the influence on of crystal size and quality on the sensitivity of the explosives. Initial compositions were made with a solid load of 85wt% RDX. The mechanical properties were varied by means of a chain extender binder and by changing the amount of plasticizer (IDP). Unfortunately, casting of the first series of composites was extremely difficult.

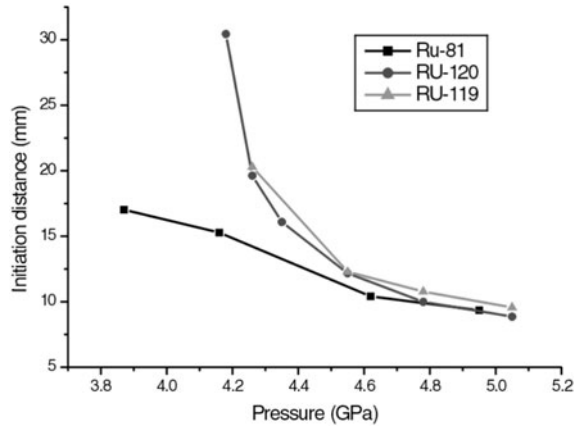


FIGURE 1. An overview of the Gap-test results. The compositions RU-119 and RU-120 with chain extender in comparison with the reference Ru81.

Subsequent RDX-PBX formulations considered, were made with only 80%wt solid load and a binder system with chain extender and 15 and 30% IDP. Two compositions were selected that were castable, RU119 and RU120, and tested in the friability apparatus⁹, shock sensitivity and cook-off test and compared with the reference RU 81 (85%wt RDX and no chain extender) and HU-28 (85%wt HMX). These PBXs were stiffer than the reference materials. This seemed to have a positive influence for the results in the friability test⁹. These materials were damaged by a 150 m/s impact and then reacted in a closed combustion bomb. The pressurisation rate of the RU120 was observed to be 5.8 MPa/ms whereas the stiffer formulation Ru-119 experienced a rate of 2.2MPa/ms. A comparison of an 80% solid load RDX-PBX was not done. In the cook-off test, no difference in reactive behaviour was observed, for the shock sensitivity by means of a flyer impact test, a small difference was shown8.

Because it is empirically known that RDX-PBXs are more thermally sensitive than HMX, HMX was used in the next series of compositions. The mechanical properties were varied systematically controlling the molar ratio of the chain extender (Trimethylhexanediol) and the prepolymer hydroxyterminated polybutadiene (HTPB). These ratios were respectively, 2.5, 1.25, 1.75 for the HU-39, HU-40 and HU-41. For the final composition HU-43 or HU-44 (different batch of HMX) a ratio of 1.5 was selected, based on the Young's moduli and the mechanical damage observed in the friability test. The bimodal mixture of HU-43, has a main particle size of two composing HMX grades being about 16 and 350 μm and a density of about 1.57 g/cm³.

MECHANICAL PROPERTIES AT HIGH STRAIN RATES

Prior to laboratory-scale testing of sensitivity, the mechanical properties of HU-43 have been measured extensively using a Zwick 1445 and a Zwick 1852 drawbench. The Zwick 1445 elongates the HU-43 samples at a speed of 50 mm/min, at temperatures of -60, -40, -20, 20 and 60°C. With the Zwick 1852, the HU-43 samples are elongated at speeds of 0.001, 0.01, 0.1, 1 and 5 m/s, and at temperatures of -40 and +20°C. The stress-strain curves of HU-43 at different temperatures and strain rates respectively, are displayed in figures 2a and 2b.

It is observed that the Young's modulus decreases from $2.1 \cdot 10^8$ Pa to $4.2 \cdot 10^6$ Pa as the temperature changes from -60° C to $+60^{\circ}$ C. The maximum attainable deformation of HU-43 before mechanical failure occurs, strongly depends on temperature. No strong influence on maximum strain is observed at the varies deformation rates. The somewhat strange upper curve in

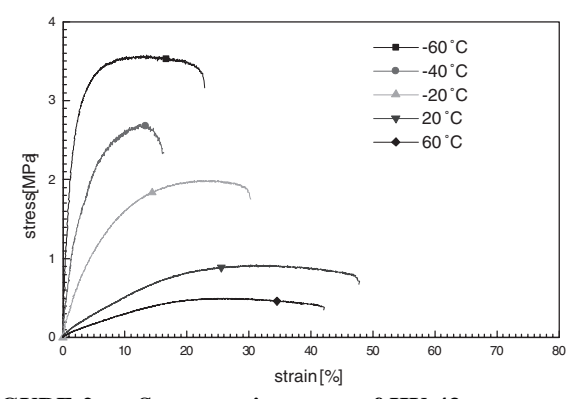
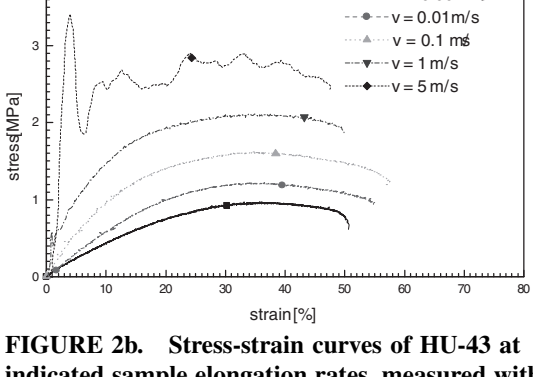


FIGURE 2a. Stress-strain curves of HU-43 at indicated temperatures, measured with the Zwick 1445 and sample elongation rate of 50 mm/min.



v = 0.001 ms

FIGURE 2b. Stress-strain curves of HU-43 at indicated sample elongation rates, measured with the Zwick 1852 at 20°C.

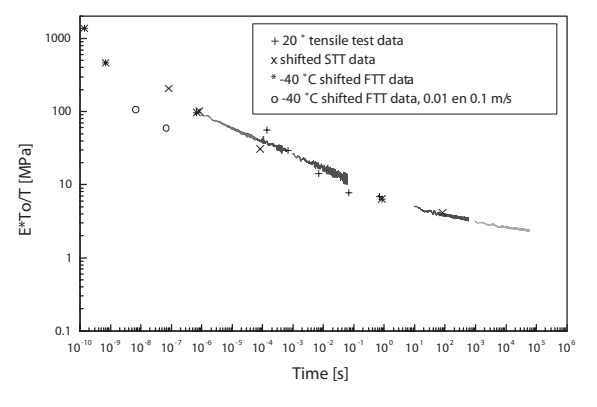


FIGURE 3a. The temperature shifted master curve of HU-43 together with the values of the tensile strength test.

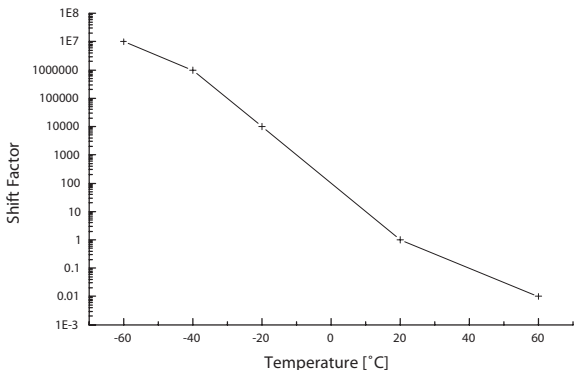


FIGURE 3b. The shift factors as a function of the temperature for HU-43.

figure 2b, corresponds to an elongation rate of 5 m/s which is the limit of the rheometer. At 20° C the Young's modulus increases from 6.8 to $29.5 \cdot 10^6$ Pa, with an increase in sample elongation rate from 0.001 to 1 m/s. The strain rates corresponding to 0.001 and 1 m/s are 0.0125 and $12.5 \, \text{s}^{-1}$.

Relaxation testing has also been performed on HU-43/44, in the range of -60°C to $+60^{\circ}\text{C}$. The relaxation test results have been analysed and shifted to obtain the so-called temperature corrected master-curve for HU-43, as shown in figure 3a. In the figure, the Young's moduli at different temperatures (see figure 2a and 2b) have been incorporated, using the shift correction of figure 3b. A good correlation between the relaxation results and the drawn-bench results is observed. With these results, the material properties of HU-43/44 at very high deformation rate can then be used in hydrocode simulations of the gas gun experiment in which material is damaged by a 150 m/s impact.

MECHANICAL DAMAGE AFTER IMPACT IN A GAS GUN EXPERIMENT

Following mechanical characterisation, HU-43 samples of 9 grams and 18 mm diameter were damaged by impact against a steel plate. Velocities in the range from 91 to 154 m/s were examined. The samples were inspected, by means of visual inspection (microscopy), observation of the actual impact process with a high-speed camera recording and analysis with scanning electron microscopy.

Visual Inspection

The fragments of HU-43 after impact on steel were collected and the damage was visually examined to assess the sensitivity of the explosive substance to deterioration by impact. An optimal composition of an HMX-PBX has been established (HU-43) by improving the resistance to

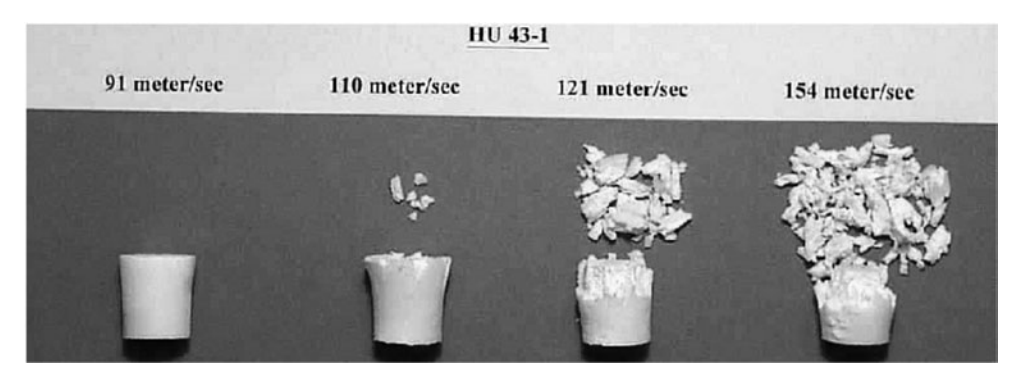


FIGURE 4. Fragments of HU-43 collected after firing bare cylinders on a steel plate at indicated velocities.

mechanical deterioration, by systematic variation of the molar ratio of the chain extender as mentioned before.

Figure 4 displays the damage of HU-43 by impact at different velocities. At 91 m/s impact velocity, it is observed that the cylindrical charge, expands in diameter at the impact side. At 154 m/s a large number of fragments are formed at the impact side, which appear to 'peel off' at the outer radius, leaving a cylindrical core. The mass lost in fragments (measured as the difference of initial mass, i.e. 9.0 ± 0.1 g, minus the mass of the largest piece collected after the impact) correspond to 0.0, 0.1, 2.0 and 3.8 g for impact velocities of 91, 110, 129 and 154 m/s, respectively.

High Speed Film

The impact of HU-43 on steel has been observed using a Hycam high-speed camera, with a 40,000 fps framing rate. A selected frame of a typical test is shown in figure 5, at 145 m/s impact velocity. Background light is used to create a shadow picture, and the optical axis of the camera is aligned parallel to the steel plate. In the picture below the left boundary of each frame corresponds to the steel plate and the explosive cylinder is coming from the right. In the subsequent frames the sabot is evident. Extensive deformation of HU-43 is observed at impact, followed by fragmentation at the impact side, resulting in a fragment spray that blurs the location of the steel plate and the cylindrical charge. Furthermore, considerable kinetic energy is dissipated by the intense fragmentation,

and it takes a relatively long time before the HU-43 core rebounds.

At lower impact velocities the deformation process (elastic and plastic) is readily observed including impact and rebound.

Numerical Simulations

Numerical simulations have been performed with the hydrocode Autodyn. Preliminary numerical simulations have already demonstrated that the incorporation of strain-rate dependent mechanical properties are necessary, see also reference 1. The mechanical properties displayed in figures 2 and 3 have been extrapolated and implemented in a subroutine for Autodyn calculations.

In the linear visco-elastic regime the mechanical properties of a substance are described by three different moduli: the compression, tensile and shear modulus. The tensile or Young's modulus is measured. The compression modulus is not incorporated in Autodyn, but a shock-Hugoniot $U_s=2.712+2.36\cdot u_p$ based on a simple rule-of-mixture applied to sound velocity and slope S, and weight fraction of HMX and binder was included. The Gruneisen coefficient is assumed to be 1.3 by read across of other PBXs. The shear modulus is set equal to 1/3 the strain-dependent Young's modulus.

An erosion model, not to be confused with the failure model, is set up in this numerical simulation with a Langrange grid, in order to avoid problems in the computation process. When a cell has grown to 10 times



 \leftarrow direction of sample time $t \rightarrow$

FIGURE 5a. Impact of 9 gram, 18 mm diameter HU-43 cylinder on steel, at an impact velocity of 145 m/s.

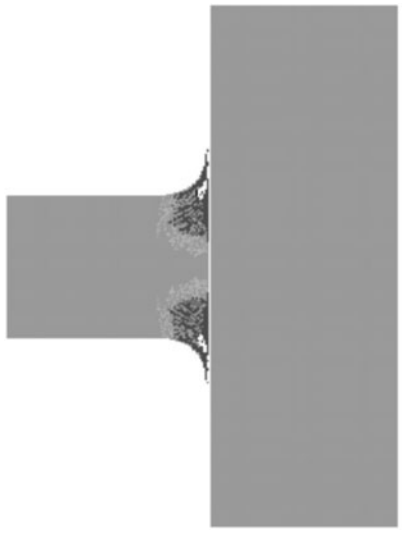


FIGURE 5b. Numerical simulation of HU-43 impacting steel at a velocity of 150 ms⁻¹.

its original size, the cell is discarded and its mass is distributed to neighbouring cells.

Figure 5b displays an example of the numerical simulation at an impact velocity of 150 ms⁻¹, at the moment of the occurrence of the central core. Various simulations have been performed to match the result of the simulation with the remaining rear part of the cylindrical samples in the impact experiment as displayed in figure 4. The results look very promising but until now a perfect match has not yet been obtained. Future simulations will be focussed on the simulation of tensile strength tests of these materials.

Scanning Electron Microscopy

Pristine and damaged HU-43 samples have been examined using a Scanning Electron Microscopy (SEM).

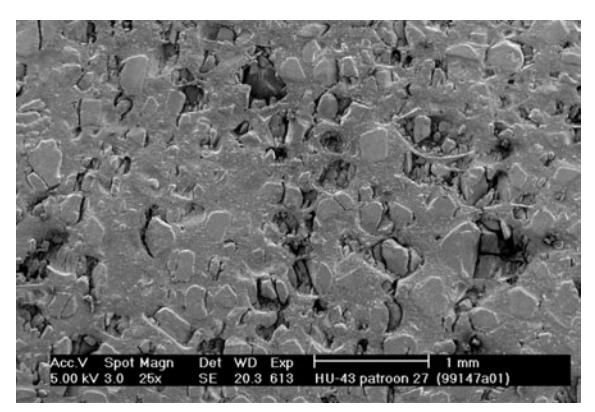


FIGURE 6a. SEM of HU-43 sample near the impact side, impact velocity is 92 m/s.

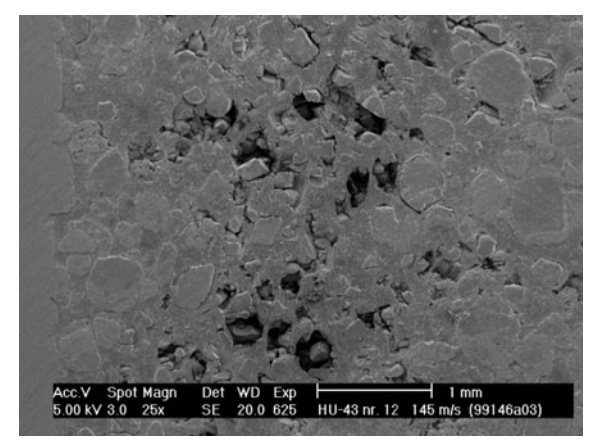


FIGURE 6b. SEM of HU-43 sample near the side opposite to impact, impact velocity is 145 m/s.

Figures 6a and 6b display the electron micrographs for samples damaged at 92 and 145 m/s, respectively. Even though the sample of figure 6a has not fragmented in the impact experiment, it is observed that the HMX crystals contain much damage, and are broken up into smaller crystals. The same effects are observed at the rear side of the sample in figure 6b.

Figure 7 displays the SEM's of the binder corresponding to the sample with a 92 m/s impact velocity. The magnification is larger than in figure 6. Near the rear side no difference with the pristine sample is observed. However, in the centre of the sample, elongation of the binder, and debonding of HMX from the binder, is observed. This corresponds to that part of the sample that is deformed plastically. The location of extensive deformation can be clearly defined in the highspeed film recordings in figure 5.

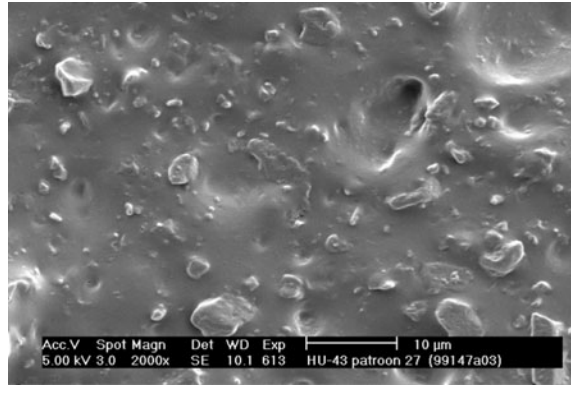


FIGURE 7a. SEM of HU-43 sample near the rear side, impact velocity is 92 m/s.

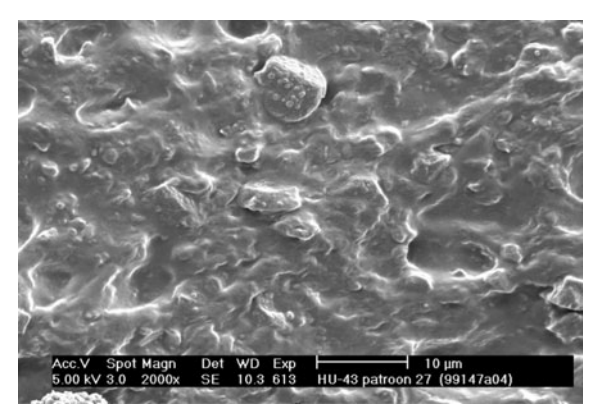


FIGURE 7b. SEM of HU-43 sample near the impact side, impact velocity is 92 m/s.

Shock Initiation

The shock initiation thresholds of pristine and mechanical damaged HU-43 have been determined by flyer impact. The initiation threshold is determined in a series of 8 samples. The damaged samples have been prepared by impact at about 150 m/s. The initial mass of those 8 samples is 9.00 \pm 0.08 gram, the impact velocity of the samples is in the range 146.0 to 151.9 m/s, and the mass of the remaining core is in the range 4.70 to 5.58 gram.

The rear side of the damaged sample is impacted by a 125 μm thick Kapton foil. The thickness of the flyer is relatively small, the mean particle sizes of bimodal mixture of HU-43 and are 16 and 350 μm . It means that if a difference in shock initiation threshold with this flyer thickness is observed, the difference in shock initiation in a gap test will probably be even more distinct.

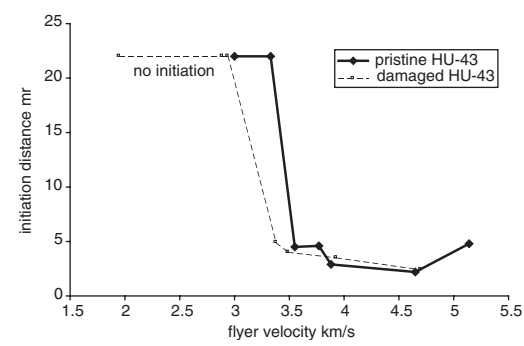


FIGURE 8. Initiation distance vs. flyer impact velocity of pristine and damaged HU-43.

To access the shock-to-detonation transition, or the failure of initiation, a fibre optic probe is inserted in the sample ¹⁰.

The initiation distance of pristine and damaged HU-43 is given in figure 8 as a function of the flyer impact velocity. The initiation threshold corresponding to pristine and damaged HU-43, at an impact of a 125 μ m Kapton flyer between 3.33 and 3.55 km/s, and between 2.94 and 3.38 km/s. It is clear that the damage influences the initiation-noinitiation threshold.

QUANTIFICATION OF DAMAGE, A NEW APPROACH

Damage can be induced by means of a thermal threat (cook-off), a mechanical threat (bullet impact) or a combination of both (hot fragment impact). Damage leads to a specific response of the explosive that at this time is not well understood. Damage is, among other things, a combination induced porosity, change of the binder properties, deformation of the binder, debonding of the binder from the crystals, crystal cracks, and phase change of the crystal material. All these effect need to be implemented in an attempt to set-up a damage model.

The amount of damage can also be determined by macroscopic measurement such as pressurisation rate in a closed combustion bomb (for thermal damage) or by the change of amount of work under a stress-strain curve (for mechanical damage). TNO-PML has developed a test plan to relate the amount thermal and mechanical damage, to the response in an IM threat, such as shock initiation or fragment impact test. Additionally, the thermal damaged will also be related to the mechanical properties of the damaged material compared to the pristine material.

To determine the thermal damage, the material is subjected to elevated temperatures of $\sim 170^{\circ}\text{C}$ for several hours and used in a Flyer impact test (SDT) and a fragment impact test. The mechanical properties are then measured by means of a gas dilatometry test⁴. To quantify the amount of damage, closed combustion bomb testing is performed.

To induce a quantified amount of mechanical damage, a Load-Unload cycle experiment is performed in a draw-bench. Due to the foregoing load, the material has lost a part of its reinforcement (reduced stiffness). Therefore the material exhibits hysteresis behaviour. The area in between the two consequent loading curves defines the amount of damage in the material (figure 9). After mechanical damage, shock initiation testing and closed bomb testing is performed, to relate the mechanical damage to the closed vessel parameters and, hopefully, fragment impact testing.

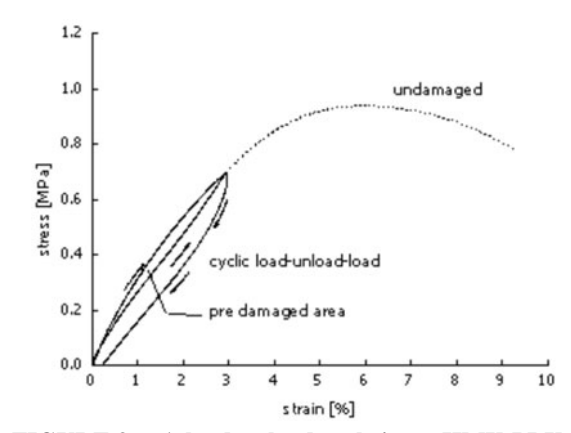


FIGURE 9. A load-unload cycle in an HMX-PBX, giving a quantitative amount of mechanical damage to a sample.

FIRST RESULTS OF THE NEW APPROACH

Change of Mechanical Properties at High Temperatures

As seen in figure 2a, the strength of a composite such as HU-43 drops significant at elevated temperature. To determine how the mechanical properties change as a function of the temperature, tensile strength tests have been performed up to a temperature of 140°C. In this test series, the samples were held at a constant temperature for 1 hour before the tensile strength test was performed. The results are shown in the figures 10. From the figures, it is clear that the mechanical properties drop significant and with the initial modulus and material strength almost dropping to zero at a temperature of about 120°C. The strain at maximum strength, increases up to a temperature of 60°C and drops above this temperature. The strain at rupture also increases up to a temperature of 60°C, drops above this temperature but increases again after 80°C.

Gas Dilatometry Testing (GDM)

Gas dilatometry combined with tensile strength testing, produces much insight in to the damage process of HTPB-binder systems. As described extensively in reference 4, the damage process consists of 4 stages. First, the visco-elastic response phase, secondly, the polymeric chain failure, the third phase, dewetting (dilatation) and finally, macroscopic failure. Hence failure of composites consists of a highly complex, time-temperature dependent behaviour. Compared to the polymeric binder, the solid load particles result in a reinforcement of the material (increased modulus). Failure of the composite, initiates early in the stress-strain history. Stress concentrations in the vicinity of filler particles, results in a local failure of the polymer chains (polymeric chain failure, slippage and polymeric reorientation). After sufficient micro-structural damage, vacuoles form and grow with continued straining. Depending on the nature of the polymer-filler bond, this vacuole spreads to the interface and unbonds the particle (dewetting). When binder and the filler are strongly bonded, vacuoles appear to stay entirely in the polymer phase. After further growth of the vacuoles, cracks form resulting in a failure of the composite. In fast compression testing or bullet/fragment impact tests, cracking of the explosive crystal also occurs, as revealed in the SEM photographs of figure 6 and 7.

In a load-unload cycle, damage by the polymeric chain failure, occurs at rather low strain levels (see figure 9, shown by the change of path of two consequent loads, the pre-damage area). The forming of vacuoles start at higher levels, as is shown in figure 11b (deviation from zero). However, a direct partial rehealing of damage is possible in this kind of composite. A recovering time of \sim 2 weeks at 50°C, can result in an almost virgin composite.

To analyse the influence of an elevated temperature on the damage process, samples of HU-44 are held at a temperature of 120 and 160°C and then tested in the

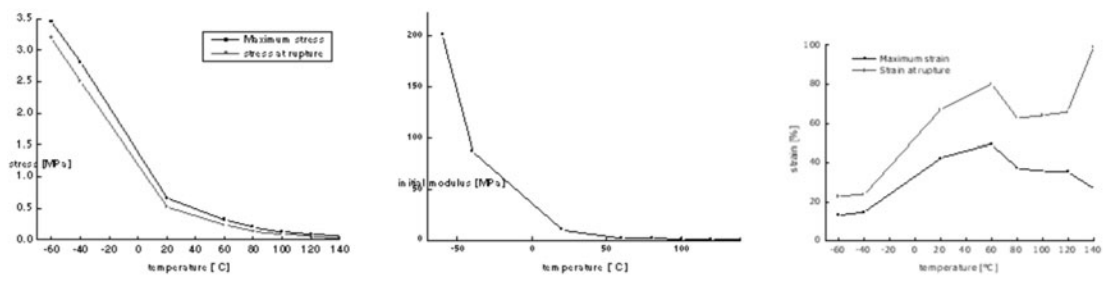


FIGURE 10a, b, c. Mechanical properties of HU-44 after 1 hour at indicated elevated temperatures. In figure a, the maximum stress and stress at rupture is given in, b, the initial modulus and in figure c, the maximum strain and strain at rupture.

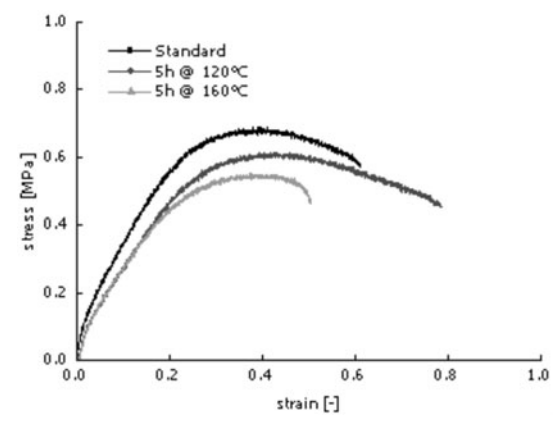


FIGURE 11a. The strain-strain curves in a GDM of samples held at a temperature of 120 and 160°C, for 5 hours, in comparison with pristine material.

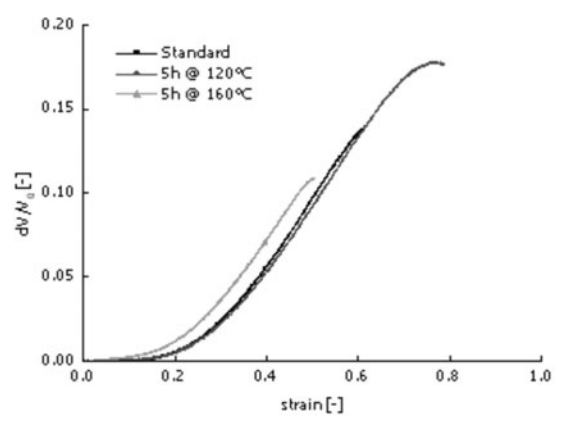


FIGURE 11b. Dilatation behaviour of samples held at 120 and 160°C, for 5 hours, in comparison with pristine material.

GDM. The results are compared with the pristine material. The results of the GDM test are shown in figure 11a and 11b. From figure 11a, one can see that the initial modulus slightly changes compared to the pristine material, resulting in a softer material and up to a strain of about 10%, little differences are seen between the 120 and 160°C samples. The maximum strength has changed slightly. Figure 11b, shows no change in the dilatation behaviour between the pristine and damaged sample at 120°C. However, for the sample damaged at 160°, the curve almost immediately starts rising, indicating that damage in form of vacuoles were formed during the heating process, probably an increase of the porosity.

Thermally Damaged Samples

Before testing in the closed vessel, Flyer impact and GDM, samples were thermally damaged at several elevated temperatures. The Bam Friction and Fallhammer

test [9] of a sample heated at 170°C indicates that the material is quite sensitive (144N and 4 Nm respectively, in comparison with >360N and 20 Nm for pristine material and 324N and 10 Nm for damaged material, for 5 hours at 160°C). In figure 12a, the sample are displayed and compared to the pristine material. It is clear that an oxidation process has been taken place, shown by the darkening of the samples. Compared to the pristine material the samples that were held at 165°C, for 5 hours, showed a sample mass loss of 0-0.05 g, at 170°C a 0.1 g and at 175°C 0.25 g mass loss. Also the form of the cylinders changed due to the heating. The GDM samples also became longer compared to the pristine material. In the magnification of the sample at 175°C (figure 12b), cracks are shown indicating a high level of damage has occurred already during heating. This type of damage will probably have a major influence on the sensitivity of the explosive, which will be revealed by the experiments performed in the next test series.



FIGURE 12a. Thermally damaged samples of temperatures of respectively 165, 170 and 175°C (for 5 hours) compared to pristine material.



FIGURE 12b. Magnification of one of the samples showing cracks after thermal heating.

Shock Initiation Testing

The thermally damaged samples have not yet been fully characterised in the flyer impact test to determine the effect of damage on the shock sensitivity. However, the first test series reveals that the detonation velocity drops rather strongly from 8.3 km/s for the pristine material to 7.0 km/s for the damaged material at 175°C (figure 13).

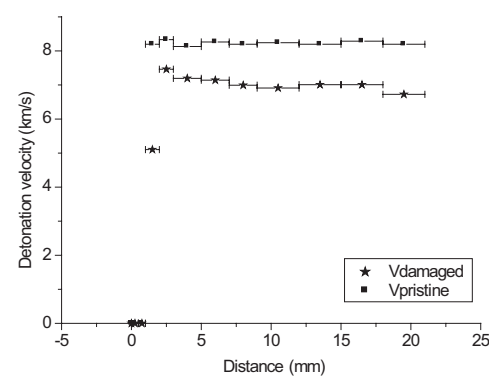


FIGURE 13. The detonation velocity of a damage (5, hours at 175°C) in comparison with a pristine HU44 sample measured with a fibre optic probe.

Fragment Impact Testing

Fragment impact testing was performed on pristine as well as on thermally damaged material. The test was performed with a cylindrical tungsten fragment of 70 g and a diameter of 22.1 mm and a test vessel made of 34Cr-NiMo6V steel with a static burst pressure of $\sim \! 100$ M Pa and the cap thickness of 5 mm. The go-no-go threshold of the pristine material was between a fragment velocity of 500-532 m/s. At 500 m/s no reaction occurred and the fragment was even stopped by the explosive material At 532 m/s a prompt shock was observed.

To perform a fragment impact test on a thermally damaged material, the test vehicle was heated using an electric heater over the total length of the vessel. The maximum temperature of a vessel of this size is about 165°C, resulting in an estimated temperature inside the vehicle of 156°C and a few degrees higher. A higher temperature results in a runaway of the explosive. Before impacting, the material was heated for 5 hours at the prescribed temperature. At a velocity of 472 m/s, no reaction occurred and partly decomposed and thermally damaged material was found all over the test bunker. At 511 m/s a detonation was observed. This value falls in-between the go-no-go threshold (500-532 m/s) of the pristine material so a difference in sensitivity is not yet apparent at this temperature. Looking at the GDM test results at 160°C for 5 hours (figure 11), this could probably be expected.

DISCUSSION AND CONCLUSIONS

The first results of the research into changes of mechanical properties of HMX and RDX PBXs in relation to sensitivity testing of thermally as well as mechanically damaged materials has been summarised in this paper. Already from the first test series with RDX-PBX, is could be concluded that the change of mechanical properties had a major influence on the sensitivity of the explosive, in particular in the friability and the Gap test. A new reference explosive, HU-43/44 was subsequently developed for research purposes and mechanically characterised. Mechanically damage HU-43 samples were submitted to visual as well as SEM inspection and also to shock initiation testing. Several types of damage were found like, deforming of the binder and reorientation (Polymeric chain failure), vacuole forming and debonding of the binder from the crystal and crystal fracture. The results of the computer simulation of a impact test are very promising but the model still needs improvement.

To quantify the amount of damage and find a relation between amount of damage and the sensitivity of an explosive a new approach was devised. The first results indicate that for mechanical damage, rehealing can occur. Thermal damage is caused by oxidation processes beginning at temperature of about 150°C and result in a irreversible type of damage. At 120°C for 5 hours, a slight change of mechanical properties was found. At a temperature of 160°C, for 5 hours, the dilatation test results indicated just a small increase of vacuoles. Also, the Bam friction and Fallhammer test, did not reveal an large increase of sensitivity of the damaged material. The fragment impact tests, performed with thermally damaged material below and up to 160°C, indicated no increase in sensitivity, compared to the pristine material.

However, at 170°C, the Bam friction and Fallhammer test, indicated that the damaged material was relatively sensitive. The first shock initiation tests series with thermally damaged material (175°C for 5 hours) revealed a drop in the detonation velocity from 8.2 to 7.0 km/s indicating a major change of the material. A conclusion about a change in sensitivity can only be made after a full characterisation of the damaged material. It seems that the increase in sensitivity, due to thermal damage, starts between 160 and 170°C due to the oxidation of the binder and decomposition of HMX leading to a porous and brittle material.

A first start has been made to reveal the complex phenomena of damage, to quantify damage and to set up a relation between the amount of damage, mechanical properties and the increase in sensitivity for several IM stimuli. But much work still needs to be done.

REFERENCES

1. R. Heiser, K. Wolf, Numerical simulation of the deformation of propellant grains under dynamic loading, 28th International Annual Conference of ICT, June 24–27, Karlsruhe, Germany.

- 2. F. R. Christopher, J. C. Foster Jr., L. L. Wilson, H. L. Gilland, The use of impact techniques to characterize the high rate mechanical properties of plastic bonded explosives, 11th International Detonation Symposium, August 31–September 4, 1998, Snowmass, Colorado, USA.
- 3. H. P. Richter, L. R. Boyer, K. J. Graham, A. H. Lepie, N. G. Zwierzchowski, Shock sensitivity of damaged energetic materials, Ninth Symposium (International) on Detonation, 1989, Portland, Oregon, USA.
- 4. H. L. J. Keizers and D. Tod, Cumulative damage of rocket propellants.
- 5. STANAG 4439, Policy for introduction, assessment and testing for insensitive munitions (MURAT).
- 6. AOP 39, Guidance on the development, assessment and testing of insensitive munitions (MURAT).

- 7. R. H. B. Bouma, A. C. Hordijk, J. H. G. Scholtes, Relation between damage at low velocity impact, and mechanical properties and explosive loading of plastic bonded explosives, 29th International Annual Conference of ICT, June 30–July 3, 1998, Karlsruhe, Germany.
- 8. J. H. G Scholtes, Onderzoek naar de variatie van mechanische eigenschappen van HTPB PBX-en, Internal TNO-PML report, May 1995.
- 9. UN Manual of Test and Criteria, Transport of Dangerous Goods.
- 10. W. C. Prinse, R. J. van Esveld, R. Oostdam, M. P. van Rooijen, R. H. B. Bouma, Fibre optical techniques for measuring various properties of shock waves, 23rd International Congress on High-Speed Photography and Photonics, September 20–25, 1998, Moscow, Russia.